解　説

表面科学 Vol. 18, No. 2, pp. 108−115, 1997

Remote Plasma Deposition of a-SiC:H Films Using Novel Source Material

Sunil WICKRAMANAYAKA, Alexander M. WROBEL* and Yoshinori HATANAKA**

Anelva Corporation, 5−8−1 Yotsuya, Fuchu, Tokyo 183
*Polish Academy of Sciences, Center of Molecular and Macromolecular Sciences, Sienkiewicza 112, 90−363 Lodz, Poland
**Research Institute of Electronics, Shizuoka University, 3−5−1 Johoku, Hamamatsu 432

(Received September 27, 1996)

An investigation of the deposition of a-SiC:H films in a remote H plasma environment using tetramethylsilane, hexamethyldisilane and tetrakis(trimethylsilyl)silane was carried out. All these monomers produce a-SiC:H films in the presence of atomic hydrogen. The stoichiometry and E_{opt} of the films deposited are found to depend on the substrate temperature. All the films deposited show photoluminescence (PL) when excited with 325 nm laser light. Films deposited at room temperature shows a blue-white PL. The PL intensity drops with an increase of substrate temperature used for the deposition. Further a red shift of the PL is observed with an increase of substrate temperature. In addition, a reaction scheme for the film formation is modeled through the generation of $Me_2Si{=}CH_2$ precursor.

1. Introduction

The growing interest in the investigation of electrical and optical properties of amorphous semiconductor films prepared by plasma polymerization is connected not only with the cognitive aspects but also with the applications in microelectronics industry. For example, with the success of valence controllability of a-SiC:H films prepared by plasma enhanced CVDs[1,2], the fields of applications of this tetrahedrally bonded material have been widen into various electronic and opto-electronic devices such as thin film transistor, photo-receptor, X-ray and color sensors. Since there is not a long-range ordering or structural symmetry of these amorphous materials, various kinds of film compositions can be realized having different electronic properties. The absence of long range periodicity also relaxes the k-selection rule[3] for the optical transition, therefore, a higher luminescent efficiency can be expected.

The first article on the fabrication of a-SiC:H by a glow discharge plasma chemical vapor deposition was reported by Anderson et al[4]. In most of the works on the fabrication of a-SiC:H films reported in the literature, SiH_4/CH_4 or SiH_4/C_2H_2 gas mixtures diluted in H_2 were used[1,4~7]. However, a major problem in the use of SiH_4 as an Si source is the necessity of a carefully designed safety precautionary tubing system combined with expensive leak detectors, because of its high pyrophoric nature. Therefore, the search for novel source monomers which are neither pyrophoric nor toxic for the fabrication of a-SiC:H is of importance. Some recent publications report the deposition of a-SiC:H film by using relatively novel carbosilane monomers such as tetramethylsilane[8], trimethylsilane[9], disilylmethane[10], disilane[11] etc. The other advantage of these materials is that these precursor gases can be used as silicon and carbon sources; therefore, the use of hydrocarbon gases as a carbon source is not needed.

In direct plasma depositions, there are different types of ionic and atomic states of gaseous species in addition to vacuum UV radiation. The initiation of the reaction process can be occurred by one or many of these radicals. Therefore, evaluation of reaction dynamics of a film deposition in direct plasma environment is difficult. In contrast, remote plasma environment provides better information for the evaluation of reaction dynamic involved with a film formation. The remote plasma deposition technique differs from direct plasma CVD in two major aspects. The first is that the plasma generation and film deposition take place in two spatially separated regions. Second is that the plasma is induced in an ambiance free of a source compound, unlike in direct plasma CVD, using a simple gas that is either chemically inert (for example Ar) or reactive (for example O_2). The source gas is added directly into the downstream few centimeters above the substrate surface. Therefore, source

gas or gases do not subject to plasma assisted dissociation. The selected active species generated in the plasma region are transported from the plasma region to the deposition site where the activation of a source compound is initiated. The most important properties of the remote plasma deposition are summarized below.

1. Number of the types of active species with respect to that of direct plasma CVD is substantially less. 2. The source compound can be made active either by excited atoms, radicals, or vacuum UV radiation. 3. Deposition takes place in electron and ion free environment, hence the substrate and the growing film do not get damaged by the bombarding charged particles that often occur in direct plasma CVD. 4. The chemistry of the process can be predicted and controlled.

There are a number of papers in the literature reporting the structure and properties a-SiC:H films produced by the remote plasma CVD, however, the mechanism of this film formation process is yet to be studied. Therefore, we have undertaken a systematic study of the remote plasma CVD of a-SiC:H films using tetrakis(trimethylsilyl)silane (TMSS), tetramethylsilane (TMS) and hexamethyldisilane (HMDS) as model source compounds and a reaction model for the deposition is presented. In addition the relationship between the H content and the E_{opt}, and the variation of photoluminescence (PL) characteristics of a-SiC:H films with the film composition is also discussed.

2. Experimental

Figure 1 is the schematic diagram of the experimental setup. The apparatus made of Pyrex glass consists of two major regions that are called as the glow discharge region and the downstream region. The glow discharge plasma is made by applying an rf (13.56 MHz) power through an inductive coil. Hydrogen gas was used as the upstream gas for through out the experiment. Hydrogen was fed to the flow tube with a rate of 200 sccm. The pressure inside the tube was maintained at 0.2 Torr.

To assess the roles of UV radiation and radicals for the reaction processes, three types of flow tube configurations as shown in Fig. 1 were used. When the straight-tube configuration shown in Fig. 1 (a) is used, both hydrogen radicals and UV radiation generated in the plasma region reach the deposition site. The UV radiation can be cut off from the deposition site, when the bend flow tube shown in Fig. 1(b) is used. Therefore, with this configuration the reaction process between the hydrogen radicals and the source gas can be studied. Similarly, hydrogen atoms reaching the deposition site can be eliminated by inserting a metal trap into the straight flow tube as shown in Fig. 1(c). Atomic radicals are effectively recombined on metal surfaces, for example, the recombination coefficient of

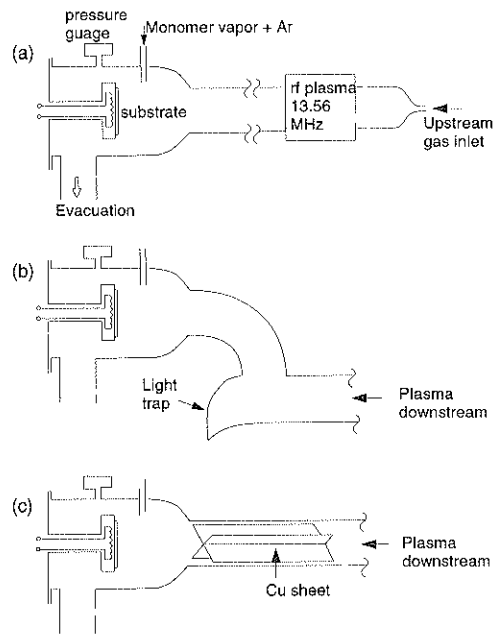

Fig. 1 Schematic diagram of the experimental set up with a) straight tube, b) bent tube and c) straight tube with metal plates inserted.

atomic hydrogen on Cu surface is 0.1[12]

Depositions of a-SiC:H films were carried out in the downstream region 60 cm below the plasma generation inductive coil. Films were prepared on c-Si(100) and quartz substrates. The source gas was introduced into the flow tube 5 cm above the substrate surface. As the source gases, TMSS, HMDS and TMS were used. HMDS and TMS are liquid at room temperature, therefore, a bubbler was used with He as the purging gas in obtaining their vapor phase. Since TMSS is a solid at room temperature, the sublimation process was carried out at 70 °C in obtaining vapor state of TMSS. The sublimated TMSS vapor is purged with He gas into the flow tube. He flow rate used for purging the above source monomers into the flow tube was kept at 10 sccm.

Films deposited on Si substrates were used for FTIR, ellipsometer, XRD, Auger emission spectroscopic and PL measurements while films deposited on quartz glass were used for the optical absorption measurements to estimate the optical band gap (E_{opt}). The E_{opt} was estimated by plotting $(\alpha h\nu)^n$ against $h\nu$ which is usually called as Tauc plot[13] in which α is the absorption coefficient and $h\nu$ is the photon energy. Since the deposited films showed dielectric properties, $n = 1/3$ was used for the E_{opt} calculations[14].

The concentration of hydrogen radicals at the reac-

tion site was estimated by nitric dioxide titration technique[15]. Measurements of film thickness were performed by ellipsometrically using an ellipsometer.

The hydrogen content of the a-SiC:H films deposited was evaluated by using the transmission FTIR spectra of the deposited films. Hydrogen bonded to Si and C was separately estimated using the wagging mode vibration of Si-H at 640 cm^{-1} and stretching mode vibration of C-H_n ($n = 1, 2, 3$) at 2965 cm^{-1}. The values of oscillator strength of Si-H and C-H_n vibrations were obtained from literature[14, 16]. Detailed information on this calculation process is given in previous reports[14, 16~18].

The PL measurements have been performed using a 325 nm He-Cd (20 mW/cm^{-2}) laser. The PL detection system was consisted of a monochromater, a lock-in-amplifier, a photomultiplier tube and a recorder. All the PL measurements were carried out at room temperature and corrected for the spectral sensitivity of the detection system.

3. Results and discussions

3. 1 Characterization of film composition

Films obtained using TMSS, HMDS and TMS are confirmed as a-SiC:H by the FTIR, XRD and Auger emission spectroscopic measurements. However, Auger spectroscopic data point out that the existence of small amount of oxygen (<4 %) in the deposits. Regardless of the substrate temperature, this oxygen content is found to be nearly a constant. There may be three possible reasons for this oxygen contamination as; 1. the desorption of surface-adsorbed H_2O and other impurity gases, 2. etching of Pyrex surface by hydrogen atoms and 3. micro-scale leaks or dead space in the tubing systems.

Figure 2 shows the FTIR spectra obtained for a-SiC:H films deposited with HMDS at different temperatures. The other source monomers, TMSS and TMS, also show similar FTIR spectra for a given temperature. The two major peaks observed near 1004 cm^{-1} and 806 cm^{-1} are attributed to Si-CH_2 wagging mode vibrations and Si-C stretching mode vibrations. Also notable in FTIR spectra is the Si-CH_3 bending mode vibration at 1250 cm^{-1} that gradually decreases with an increase of the substrate temperature. Further, the spectra show several weak absorptions at 2960 cm^{-1} due to the stretching mode vibration of C-H_n ($n = 1, 2, 3$). These absorptions also reduce with an increase of the substrate temperature. Apparently, films contain a very small amount of H bonded to Si, because, the absorption related to Si-H vibrations at 640 cm^{-1} and 2190 cm^{-1} are weak. The absorbance intensity at 640 cm^{-1} related to Si-H wagging mode vibration is slightly stronger when compared to that at 1290 cm^{-1} which is related to Si-H stretching mode

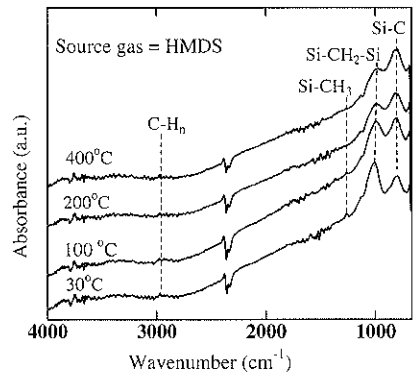

Fig. 2 FTIR spectra obtained for a-SiC:H films deposited with HMDS at different temperatures.

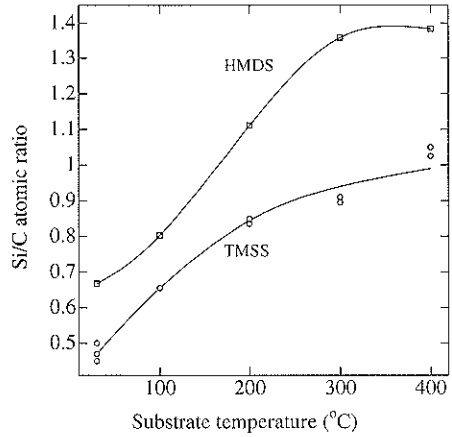

Fig. 3 Film composition of a-SiC:H films deposited using TMSS and HMDS monomers as a function of substrate temperature.

vibration. This may be due to the weaker oscillator strength of the stretching mode vibration compared to that of the wagging mode vibration[18]. The intensities of these absorbances also decrease with an increase in the substrate temperature to an undetectable level at 400 °C. However, if the films are deposited with SiH_4/CH_4 or SiH_4/C_2H_2 gas mixtures, the films show a considerably stronger absorbance at ca. 2190 cm^{-1} due to the Si-H stretching mode vibrations[6, 7, 10, 19]. The absorbance bands at 845 cm^{-1} and 880 cm^{-1} which are commonly assigned to $(SiH_2)_n$ and SiH_2 modes[10] could not be observed, we believe, because, the strength and the occurrence of these peaks are critically dependent on the deposition conditions[18].

The fractions of Si/C of the a-SiC:H films deposited with TMSS and HMDS at different temperatures were obtained by AES measurements and shown in **Fig. 3**.

All the source monomers used show a similar variation of Si/C ratio with temperature that the C fraction of the films decreases while the Si fraction goes up with an increase of substrate temperature. Almost a similar pattern of compositional variation has also been observed by previous researchers[4].

The surfaces of the films deposited are observed to be smooth and structureless regardless of the substrate temperature. The microstructure of the surface, surface free energy and chemical stability of the films deposited have been explained in detail elsewhere[20].

3.2 Effect of film composition and hydrogenation on E_{opt}

The relationship between the hydrogen content of a film and its E_{opt} is discussed using the films deposited by TMSS. However, data on the hydrogen content and the E_{opt} of the films deposited with HMDS are also shown in related diagrams. The hydrogen content bonded to Si and C has been obtained from the integrated absorbencies of Si-H and C-H_n stretching modes at 640 cm^{-1} and 2965 cm^{-1}, respectively. The wagging mode vibration of H atoms roughly normal to the Si-H bond at 640 cm^{-1} has the greatest oscillator strength of all the Si-H modes[14, 18]. Therefore, only this peak is clear in the FTIR spectra and is used for the evaluation of the hydrogen content bonded to Si. The total H concentrations of the films deposited with TMSS and HMDS are shown in **Fig. 4** as a function of substrate temperature. In addition, the hydrogen content bonded to Si and C of the films deposited with TMSS are separately listed in **Table 1**. During the calculation it was observed that a higher fraction of hydrogen in the films is bonded to C. The amount of hydrogen bonded to C is nearly three orders higher compared to that of Si, however, some previous studies have reported that the hydrogen bonded to C and Si is nearly the same[10] or opposite[21] to that reported here. In those investigations, either there was hydrogen directly bonded to Si in the source monomer used[10] or reactive sputtering in a hydrogen environment[21] was used. In the TMSS monomer used in the present experiments, there is no Si-H bond, therefore we concluded that the lower hydrogen content bonded to Si is related to the absence of Si-H bond in the source monomer. The proposed reaction mechanism (see section 2.3) of the film formation with TMSS monomer also points out that there is no hydrogen incorporation to the Si-C skeleton during the film growth process. Therefore, the hydrogen bonded to Si must be newly created bonds during the deposition process and can not be explained by the proposed reaction model (see section 3.4). This H bonded to Si may possibly come from the hydrogen plasma, because we have observed that the C-H bond is less susceptible to decomposition from the atomic H or from vacuum UV radiation generated in the hydrogen plasma. If the depositions are performed in an atomic hydrogen environment, H atoms are usually embed into the growing film[7]. Some of these atoms may form bonds with Si atoms in the Si-C skeleton which results in a very low Si-H bond density in the prepared films.

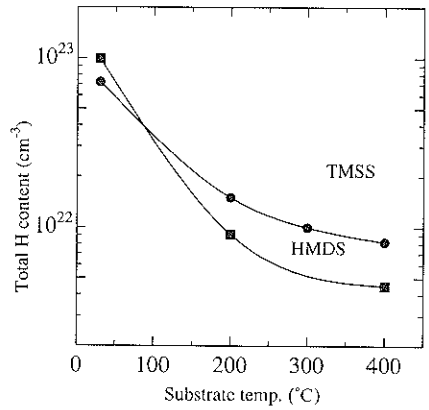

Fig. 4 Hydrogen content in the a-SiC:H films deposited using TMSS and HMDS as a function of substrate temperature.

Table 1 H atom concentration bonded to Si and C in a-SiC:H films.

Substrate temperature (°C)	N_{Si-H}($\times 10^{19}$ cm^{-3})	N_{C-H}($\times 10^{22}$ cm^{-3})
30	9.6	7.2
200	5.1	1.5
300	3.8	1.0
400	2.9	0.82

The reduction of hydrogen content with an increase of substrate temperature can assume to be consistent with the reduction of C fraction, since H in these films is mainly bonded to C. The other reason for the reduction of H with an increase of temperature is the desorption of hydrogen at higher substrate temperature. The latter consideration is not important in this case, because the removal of hydrogen bonded to C is less likely to occur at the temperatures below 400 °C. If the stoichiometry of the deposits is given as a-Si_xC_{1-x}, $x = 0.3$ was obtained for the film deposited at room temperature. This is slightly higher than the value obtained by Munekata and co-workers[22] for a film deposited at room temperature. They have estimated $x = 0.2$ for the a-Si_xC_{1-x}; H films deposited by TMS as the source gas in a glow discharge plasma. The relatively higher Si fraction obtained in the present work may be attributed to the higher Si:C ratio of the TMSS monomer (1:2.4) compared to that of TMS (1:4).

The E_{opt} estimated for the films deposited by TMSS and

HMDS are shown in **Fig. 5**. For the following discussion however, only the E_{opt} related to TMSS is considered to make the discussion simple. Some studies have pointed out that the variation of Si/C ratio influences the E_{opt}[23]. There can be two major reasons for this which are 1. the changing of bond structure with the variation of Si:C composition and 2. the influence of the type and the amount of existing bonds due to different bond strengths of Si-Si (76 kcal/mol), Si-C (104 kcal/mol) and C-C (144 kcal/mol) bonds. Therefore, with the increase of C content of the film, E_{opt} is expected to increase due to the increased density of strong C-C bonds, however, the optical gap, 3.2 eV estimated for the film deposited at room temperature seems to be comparatively high despite its lower C fraction. The E_{opt}, measured by Munekata and co-workers[22] is 2.8 eV for the film with $x = 0.2$. Therefore, our measurement is seen to be inconsistent with data reported by other researchers[22] if only the variation of E_{opt} is occurred by the variation of Si and C fractions are concerned. Hence, the formation of localized states and its influence on E_{opt} is considered next. It is suspected that a large number of unoccupied dangling bonds are introduced to the film during the film growth process. At low temperatures these dangling bonds are passivated by termination with H; however, the density of these trap states is expected to grow with an increase of substrate temperate. This is because H begins to desorb from the film with an increase of substrate temperature leaving unoccupied dangling bonds on the growing surface. The occurrence of this process is further supported by the rise of Si content in the film with temperature, since H bonded to Si is more easily removed compared to H bonded to C. This causes an extension of the density-of-states tail and thereby a decrement of effective E_{opt} with an increase of substrate temperature. Therefore, we assume that the amount of H in the film fabricated in this experiment is higher compared to that of the film made by Munekata and co-workeres[22] even though they have not reported the hydrogen content in their films.

3.3 Photoluminescence properties

The literature reports different PL spectra for the a-SiC:H films. For example, Engemann, Fisher and Knecht[24] have reported PL spectra having two major peaks and a variation of intensities of these two peaks with the film composition; however, they have also reported that the origin of these two peaks is the same. In contrast, Munekata and co-workers[22] and Sussmann and Ogden[6] have reported single peak PL spectra for which the peak position of the PL shifts toward lower energies with an increase of substrate temperature maintained during the deposition. The PL spectra obtained in the present work are similar to that of the films obtained by Munekata and co-workes[22]. **Figure 6** shows the PL spectra of a-SiC:H films fabricated at room temperature, 200 °C and 400 °C. The peak energies of the PL spectra seem to move to higher energies with decreasing substrate temperature. This result is consistent with the observed variation of E_{opt} with the substrate temperature (see Fig. 5). The intensity and the full width at half-maximum (FWHM) are slightly dropped and widened with an increase of substrate temperature. This can be explained by considering the increase of density of unoccupied dangling bonds and thereby the band-tail widths with substrate temperature as described above. These unoccupied dangling bonds function as electron and hole traps which not only reduce E_{opt} but also decrease the PL intensity because they act as nonradiative recombination centers. Further, with an increase of trap density, radiative

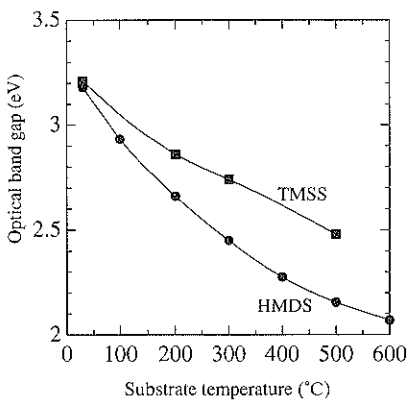

Fig. 5 Variation of optical band gap (E_{opt}) against the substate temperature. Films were deposited using TMSS and HMDS monomers.

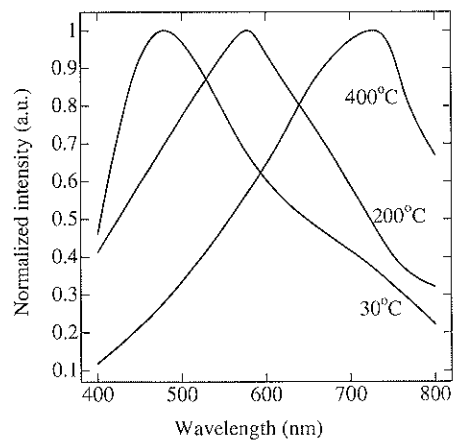

Fig. 6 Photoluminescence spectra obtained for a-SiC:H films deposited at different temperature. Films were deposited using TMSS monomer.

transitions occur over a wide energy range resulting in a broader FWHM. A detailed discussion on the relationship between hydrogenation and PL properties have been reported elsewhere[25].

3. 4 Evaluation of chemical reaction scheme of the film formation

The chemical reaction process is modeled using TMSS source monomer. The deposition rate of the film was nearly the same for straight- and bend-flow tube configurations used for a given substrate temperature. Since we could obtain a-SiC:H films with the bent tube which provides a UV radiation free environment, it can be confirmed that atomic H can activate the deposition process. In the other experiment where two Cu plates are inserted into the straight flow tube, films could not be deposited. In this case, only UV radiation exists at the reaction site to make the deposition process active since all atomic H are recombined on Cu surface. Therefore, these results point out that only atomic H can initiate the film-forming mechanism. UV radiation is proven to be ineffective for the film-forming reaction process because deposition rates observed are almost the same for both straight and bend flow tube configurations.

One or more of the three types of bonds in the TMSS molecule, Si-Si, Si-C and C-H may be susceptible to the initial break with the collision of atomic H. The bond dissociation energies of these three bonds are 76, 104, and 80.7 kcal/mol, respectively. The emission spectrum at the reaction site obtained for the straight flow tube shows the existence of H_α, H_β, H_γ atomic states which have energies of 43.6, 58.9 and 65.9 kcal/mol, respectively[26]. None of these energies is sufficient to break any of the above bonds in the TMSS molecule. When the bent flow tube is used, these H_α, H_β and H_γ radiation could not be observed, possibly due to the deactivation through collisions with the glass wall. Therefore, the decomposition of the TMSS molecule supported by a higher energy excited atomic H can be ruled out. The decomposition of the TMSS molecule, therefore, cannot be considered as a physical breakup of bonds through kinetic energy transformation of excited atomic H to source molecules, but a chemical reaction. To assure the latter conclusion, a deposition experiment was carried out using He plasma instead of hydrogen plasma in which we could not obtain any film, although He plasma makes He metastable states with energies as high as 20 eV[27].

To get a clear insight into the decomposition location of the TMSS molecule, we have carried out another deposition using CH_4 as the source gas. The results of these depositions are summarized in **Table 2**. When CH_4 is used as the source gas, a film could not be obtained even after 20 h of deposition. Further, TMS yields a film by reacting with atomic H but the deposition rate was comparatively small. With the monomers containing Si-Si bonds, films could obtain with a comparatively higher rate. These results indicate that the most susceptible bond out of the three bonds mentioned above for the participation in preliminary decomposition by atomic H is the Si-Si bond.

Table 2 Deposition rates of TMS, HMDS and TMSS source monomers in the presence of H atoms.

Monomer	Molecular weight	Considered bond	Flow rate (sccm)	Deposition rate (nm min^{-1})	Normalized deposition rate ($\times 10^3$ nm g^{-1} min^{-1})
CH_4	16	C-H	8	0	0
$SiMe_4$	88	Si-C	1	0.2	0.09
$(Me_3Si)_2$	146	Si-Si	0.5	2	1.6
$(Me_3Si)_4Si$	321	Si-Si	0.5	5.4	1.7

Literature also reports that in the gas-phase reactions of hydrogen radicals with organosilanes, the primary reaction in the activation step involves Si-Si bond[28]. The first reaction proceeds with the attachment of the hydrogen radical to the silicon atom either in the trimethylsilyl group or in a central position. Then the abstraction of tris(trimethylsilyl)silyl and trimethylsilyl radicals follows as shown below.

$$H\cdot + (Me_3Si)_4Si \rightarrow Me_3SiH + (Me_3Si)_3Si\cdot \quad (1)$$

$$\rightarrow (Me_3Si)_3SiH + Me_3Si\cdot \quad (2)$$

Reaction (1) is statistically favored, since there are four available sites for Si-Si bond cleavage to occur in the TMSS molecule. Although the contribution of the Si-C bonds to the activation step is of minor importance, as revealed by the data shown in Table II, this process may also proceeded by the attachment of hydrogen radical to the carbon atom associated with the elimination of a methane molecule.

$$H\cdot + (Me_3Si)_4Si \rightarrow (Me_3Si)_3SiSiMe_2 + CH_4 \quad (3)$$

In the secondary step, the radical structures produced in reactions (1)–(3) may undergo a reaction with TMSS.

$$(Me_3Si)_3Si\cdot + (Me_3Si)_4Si \rightarrow (Me_3Si)_3SiH + (Me_3Si)_3SiSiMe_2\text{-}\dot{C}H_2 \quad (4)$$

$$Me_3Si\cdot + (Me_3Si)_4Si \rightarrow Me_3SiH + (Me_3Si)_3Si\text{-}SiMe_2\dot{C}H_2 \quad (5)$$

$$(Me_3Si)_3Si\dot{S}iMe_2 + (Me_3Si)_4Si \rightarrow (Me_3Si)_3SiSiHMe_2 + (Me_3Si)_3Si\text{-}SiMe_2\text{-}\dot{C}H_2 \quad (6)$$

The product, $(Me_3Si)_3Si\text{-}SiMe_2\text{-}\dot{C}H_2$ of the reaction (6) may isomerize and subsequently dissociate to tris(trimethylsilyl)silyl radical and dimethylsilene[29,30].

$$(Me_3Si)_3Si\text{-}SiMe_2\text{-}\dot{C}H_2 \rightarrow (Me_3Si)_3Si\text{-}CH_2\text{-}\dot{S}iMe_2 \quad (7)$$

$$(Me_3Si)_3Si\text{-}CH_2\text{-}\dot{S}iMe_2 \rightarrow (Me_3Si)_3Si\cdot + Me_2Si{=}CH_2 \quad (8)$$

Reaction (7) and (8) are endothermic[29,30] and therefore, they may easily proceeded on a heated substrate. Moreover, trimethylsilyl radicals formed via reaction (2) may undergo disproportionation due to a relatively high value of the ratio of gas-phase disproportionation to recombination rate constants, which was found to be 0.5[31,32].

$$2Me_3Si\cdot \rightarrow Me_3SiH + Me_2Si{=}CH_2 \quad (9)$$

Dimethylsilene resulting from reactions (8) and (9) due to its biradical nature[29,30] is considered as a highly reactive film forming precursor. It can readily propagate carbosilane chain growth on the substrate surface[33].

$$n(Me_2Si{=}CH_2) \rightarrow H_2\dot{C}\text{-}(Me_2Si\text{-}CH_2)_{n-1}\text{-}\dot{S}iMe_2 \quad (10)$$

The production of dimethylsilylmethene from reaction (8) and (9) was first suggested by Fritz and Grobe[34] to explain the formation of cyclic carbosilanes as follows.

$$2[Me_2Si{=}CH_2] \rightarrow Me_2Si(\text{—}SiMe_2\text{—}) \quad (11)$$

$$3[Me_2Si{=}CH_2] \rightarrow Me_2Si(Me_2Si)(SiMe_2) \quad (12)$$

This $Me_2Si{=}CH_2$ is considered as a highly reactive precursor capable of recombining with other precursors or with the surface adsorbed radicals[35]. Therefore, this precursor is capable of forming a three-dimensional Si-C skeleton over the substrate surface via the reactions similar to reactions (11) and (12). First, $Me_2Si{=}CH_2$ radicals or partially polymerized clusters can be assumed to be absorbed by the surface. This process is supported by the dangling bonds existing on the Si surface a the beginning and even after a layer of SiC is formed. The latter is due to the abstraction of hydrogen by the bombarding atomic hydrogen. Second, the reactive carbosilane groups react with neighboring Si-CH_3 or Si-CH_2-Si groups forming larger clusters of Si-C network. Abstraction of hydrogen by the bombarding hydrogen atoms create new reactive sites for the next recombination of polymerized or non-polymerized $Me_2Si{=}CH_2$ radicals. These cross linking of carbosilane groups promotes the growth of a three-dimensional Si-C network on the substrate surface.

A similar reaction process is proposed for the film deposition with HMDS. As shown previously, the reaction starts by the dissociation of Si-Si bond by atomic H.

$$H\cdot + Me_3\text{-}Si\text{-}Si\text{-}Me_3 \rightarrow Me_3\text{-}SiH + \dot{S}iMe_3 \quad (13)$$

A similar decomposition has been reported by Davidson et al. for the pyrolysis of HMDS[36,37]. Moreover, other researchers have postulated the thermal decomposition of tetramethylsilane produces .$SiMe_3$ radical[34,38,39].

Trimethylsilane radical produced in reaction (13) then undergoes the following chain reaction process with HMDS[37,40,41].

$$Me_3Si\cdot + Me_3SiSiMe_3 \rightarrow Me_3SiH + Me_3SiSiMe_2\dot{C}H_2 \quad (14)$$

$$Me_3SiSiMe_2\dot{C}H_2 \rightarrow Me_3SiCH_2\dot{S}iMe_2 \quad (15)$$

$$Me_3SiCH_2\dot{S}iMe_2 \rightarrow Me_3Si\cdot + Me_2Si{=}CH_2 \quad (16)$$

The other interesting point in the reaction scheme presented here is that there is no hydrogen atom attached to the Si atom at any of the reaction stages. This fact may be the most possible reason for the absence of strong Si-H absorbence in the FTIR spectra. However, the H atoms usually embed into the growing film if depositions are performed in an environment of H atoms. Some of these atoms may form bonds with Si atoms in the Si-C skeleton which results in a very low hydrogenated Si atom in the a-SiC:H film.

4. Conclusions

TMS, HMDS and TMSS produce a-SiC:H films by the reaction with atomic hydrogen. The film composition and E_{opt} vary with the substrate temperature even though the overall deposition process is observed to be a temperature independent process. The Si/C ratio of the films deposited by these three monomers increases while the E_{opt} decreases with an increase of substrate temperature. The PL intensity decreases with an increase of substrate temperature due to an increase of the density of dangling bonds in the films. During the decomposition of HMDS and TMSS monomers, the Si-Si bond is the most likely bond to be broken at the first step. A reaction scheme for the deposition of a-SiC:H films is modeled using a precursor with the structure of $Me_2Si{=}CH_2$ the formation of this precursor is explained by the recombination, isomerization, and disproportionate reactions of initially generated radicals. At present, film stress and hardness of a-SiC:H films and laser assisted annealing and recrystallization are being investigated.

References

1) Y. Tawada, M. Kondo, H. Okamoto and Y. Hamakawa: Solar Energy Materials **6**, 299 (1982).
2) D. Kurangam, T. Endo, M. Deguchi, W. Gung-Pu, H. Okamoto and Y. Hamakawa: Optoelectronics-Devices and Technology **1**, 67 (1986).
3) N.F. Mott and E.A. Davis: "Electronic Processes in Non-Crystalline Materials", 2nd ed. (Oxford University Press) p. 288.
4) D.A. Anderson and W.E. Spear: Philos. Mag. **35**, 1 (1977).
5) D.R. McKenzie, G.B. Smith and Z.Q. Liu: Phys. Rev. B **37**, 8875 (1988).
6) R.S. Sussmann and R. Ogden: Philos. Mag. B **44**, 137 (1981).

7) J. Sarai, Y. Fuji, M. Yoshimoto, K. Yamazoe and H. Matsunami: Thin Solid Films **117**, 59 (1984).
8) R. Rodriguez-Clemente, A. Figueras, S.Garelik, B. Armas and C. Combescure: J. Crystal Growth **125**, 533 (1992).
9) Y.M. Li and B.F. Fieselmann: Appl. Phys. Lett. **59**, 1720 (1991).
10) W. Bayer, R. Hager, H. Schmidbaur and G. Winterling: Appl. Phys. Lett. **54**, 1666 (1989) and reference therein.
11) S. Nomura, S. Hattori and S. Nitta: Solid State Commun. **64**, 1261 (1987).
12) A Gelb and S.K. Kim: J. Chem. Phys. **55**, 4935 (1971).
13) J. Tyczkowski, E. Odrobina, P. Kazimierski, H. Bassler, A. Kisiel and N. Zeema, Thin: Solid Films **209**, 250 (1992).
14) K. Nakazawa, S. Ueda, M. Kumeda, A. Moromoto and T. Shimizu: Jpn. J. Appl. Phys. **21**, L176 (1982).
15) M.A.A. Clyne and B.A. Thrush: Trans. Faraday Soc. **57**, 2176 (1961).
16) H. Shankas, C. J. Fang, L. Ley, M. Cardona, F. J. Demond and S. Kalibtzer: Phys. Stat. Sol.(b)**100**, 43 (1980).
17) W.A. Lanford and M.J. Rand: J. Appl. Phys. **49**, 2473 (1978).
18) E.C. Freeman and W. Paul: Phys. Rev. B **18**, 4288 (1978).
19) W.A. Nevin, H. Yamagishi and Y. Tawada: J. Appl. Phys. **72**, 4989 (1992).
20) A.M. Wrobel, S. Wickramanayaka, Y. Nakanishi, Y. Fukuda and Y. Hatanaka: Chemistry of Materials **7**, 1403 (1995).
21) H.R. Shanks, J.F. Ward and C. Carlone: J. Non-cryst. Solids **59/60**, 581 (1983).
22) H. Munekata, S. Murasato and H. Kukimoto: Appl. Phys. Lett. **37**, 536 (1980).
23) I. Watanabe, Y. Hata, A. Morimoto and T. Shimizu: Jpn. J. Appl. Phys. **21**, L613 (1982).
24) D. Engemann, R. Fisher and J. Knecht: Appl. Phys. Lett. **32**, 567 (1978).
25) S. Wickramanayaka, Y. Nakanishi and Y. Hatanaka: J. Appl. Phys. **77**, 2061 (1995).
26) "Handbook of Chemistry and Physics", 54th ed (CRC Press, Boca Raton, FL, 1973-1974) p. F-200.
27) J.H. Koltz and D.W. Setser: "Reactive Intermediates in the Gas Phase: Generation and Monitoring", ed. by D.W. Setser (Academic Press, New York, 1979) p. 151.
28) R. Ellul, P. Potzinger and B. Reiman: J. Phys. Chem. **88**, 2793 (1984).
29) L.E. Guseln'ikov and N. S. Nametkin: Chem. Rev. **79**, 529 (1979).
30) G. Raabe and J. Michl: Chem. Rev. **85**, 419 (1985).
31) S.K. Tokah and R.D. Koob: J. Phys. Chem. **83**, 774 (1979).
32) S.K. Tokah and R.D. Koob: J. Am. Chem. Soc. **102**, 376 (1980).
33) A.M. Wrobel and M.R. Wertheimer: in "Plasma Deposition, Treatment and Etching of Polymers", ed. by R. d'Agostino (Academic Press, Boston, MA, 1990) Chap. 3, p. 182.
34) G. Fritz and J. Grobe: Z Anor. Allg. Chem. **315**, 157 (1962).
35) G. Raabe and J. Michl: Chem. Rev. **85**, 419 (1985).
36) I.M. Davidson and A.B. Howard: J. Chem. Soc. Chem. Commun. **9**, 323 (1973).
37) I.M.T. Davidson, C. Eaborn and J. M. Simmie: J. Chem. Soc. Faraday Trans. 1, **70**, 249 (1974).
38) G. Fritz, J. Grobe and D. Kummer: Adv. Inorg. Chem. Radiochem. **7**, 349 (1965).
39) G. Fritz: Angew. Chem. Int. Ed. Engl. **6**, 677 (1967).
40) I.M.T. Davidson and A.B. Howard: J. Chem. So. Faraday Trans.1, **69**, 1975 (1974).
41) L.E. Gusel'nikov and N.S. Nametkin: Chem. Rev. **79**, 529 (1979).